

Radar-based observation of a lava tube on Venus

Received: 24 April 2025

Leonardo Carrer , Elena Diana  & Lorenzo Bruzzone  

Accepted: 13 January 2026

Published online: 09 February 2026

 Check for updates

Intense volcanism has played a significant role in shaping Venus's surface and geology. The existence of lava tubes (i.e., pyroducts) on Venus has been largely hypothesized but never confirmed. Being a subsurface structure, the presence of a lava tube can be revealed by a localized collapse of the roof denoted as skylight. Between 1990 and 1992, the Synthetic Aperture Radar (SAR) instrument on board the Magellan spacecraft mapped the Venusian surface. By leveraging a SAR imaging technique developed for detecting and characterizing accessible subsurface conduits in the proximity of skylights, we analysed the Magellan radar images in locations where there is evidence of localized surface collapses. Our analyses reveal the existence of a large and open subsurface conduit in the Nyx Mons region. This feature is hypothesized to be a pyroduct, characterized by a diameter of about 1 km, a roof thickness of at least 150 m and an empty void height of no less than 375 m. The conduit extends in the subsurface for at least 300 meters from the skylight.

Lava tubes, natural underground tunnels formed by volcanic activity, have emerged as scientifically significant features for planetary exploration^{1,2}. They typically originate in basaltic lava flows, where low-viscosity lava is either entrenched and crusted over or inflated in-between preexisting lava layers³. Multiple modalities have been observed for the formation of a lava tube through overcrusting^{4–6}. These modalities include (i) a solid crust is formed from the levees toward the center of a channelized lava flow; (ii) overflows grow the stream levees until an arched roof is formed over the lava flow and (iii) floating mobile pieces of crust of solidified lava coalesce into a solid roof. Another lava tube formation process is incremental inflation of cooled lava sheets by flowing hot lava⁷. Once a lava tube is formed, either by overcrusting or inflation, thermal and physical erosion contribute to further shaping the conduit. Then, if the lava supply is discontinued, a partially- or fully-drained conduit may be left. Lava tubes can be modeled as quasi-cylindrical structures², with their lower and upper sections referred to as the floor and roof, respectively. By examining the formations, structures, and mineralogical compositions within lava tubes, it is possible to gain insights into volcanic activity, lava flow dynamics, and the geological processes shaping the planetary surfaces⁸.

Beside Earth, evidence of lava tubes has been identified on other celestial bodies such as Mars^{9–11} and the Moon^{12,13}. For example,

recent research provides compelling evidence of a subsurface cave conduit beneath the Mare Tranquillitatis Pit (a lunar skylight) on the Moon¹⁴. The main evidence for postulating their existence are localized collapses of the near surface¹⁵ (i.e., skylights). Skylights are typically associated with the collapse of a lava tube roof due to gravitational and erosional forces². As a result, they enable opportunities for observing and accessing a subterranean cave system.

The existence of lava tubes on Venus is uncertain and the focus of ongoing research. While no direct evidence of lava tubes on Venus has been discovered so far, there are several clues of indirect evidence that suggest their possible widespread presence such as long sinuous features, fractures, and collapse chains^{16,17} that are often associated with them. Collapse pit chains are typically observed by optical imaging sensors. Optical images (e.g., by photogrammetry) are of great aid in locating and analyzing skylights. However, the use of satellite optical remote sensing instruments is precluded on Venus because of its thick CO₂ atmosphere. NASA's Magellan¹⁸ spacecraft was equipped with a radar system able to acquire data in different modes. One of them is a side-looking SAR mode operating in S band (2.385 GHz) that was specifically designed to study Venus' surface. SAR works by transmitting radio waves towards the surface and measuring the time it takes for the

waves to bounce back after interacting with the terrain. By processing the returned radar signals, a detailed backscattering map of the Venusian surface has been produced.

Magellan detected the presence of several pit chains on Venus^{19,20}, thus revealing one of the main indicators for the possible presence of lava tubes. A recent morphometric analysis of Venusian pits using radar-derived parameters from Magellan SAR data²¹ found that these pits exhibit extremely large collapse volumes and display striking morphological similarities to lunar pit craters. They appear as linear to curvilinear assemblages of individual craters. These chains extend from tens to several thousands of kilometers in length and are distributed across diverse Venusian landscapes. Their prevalence is particularly notable in connection with chasmata and coronae. The distinctive characteristics of these formations strongly suggest their origin in collapses induced by the removal of underlying support. This loss of support could be attributed to various causes such as the collapse of a lava tube roof, extensional faulting, or receding magma chambers. Another hypothesis proposed for Venus is that these pit chains were produced in association with underlying dyke swarms²². In this scenario, they may represent collapse features formed above laterally propagating subsurface dykes. However, the specific mechanism responsible for the generation of collapse pits on Venus remains an unresolved question¹⁶. In fact, early analyses of Magellan data suggested that a number of pit craters may be associated with collapsed lava tubes²³. This hypothesis was mainly dictated by the pits' locations and the types of terrain surrounding them, as it was not possible to discern the collapse origin by only available data on surface shape and dimension of the pits. Hence, even if plausible, the hypothesis remains unconfirmed.

Here, we investigate whether Venusian pits provide access to an empty subsurface conduit and thus could potentially be collapsed sections of lava tubes (i.e., skylights). To achieve this goal, we analyze the Magellan dataset by leveraging a recent data processing methodology for hidden cavities and lava tubes characterization and accessibility assessment from radar images^{14,24}. These recent studies demonstrate that, under suitable assumptions, the use of Synthetic Aperture Radar images acquired from spaceborne platforms enables the determination of lava tubes subsurface morphometry and the related accessibility near collapse pits on Earth²⁴ and other celestial bodies⁴. This is possible by taking advantage of the side-looking acquisition geometry of the sensor resulting in radar waves traveling within the observed skylight and being reflected by the lava tube interior.

Results

Study area and Magellan radar image analyses

The study area is located on the western flank of the Nyx Mons (Supplementary Fig. 1a). The Nyx Mons is a 362 km-diameter shield volcano²⁵. The investigated region is well-documented for its large occurrence of collapse pit chains^{26–28}. Sawford et al.²⁷ noted the existence of graben systems in the region, with some near the pit crater chains, yet not fully bounding them. However, no evidence of lava tubes has been provided.

Within this region, we focused our attention on one pit denoted as A (Fig. 1), imaged by the Magellan radar from West to East and with incidence and look angles equal to about 42.4° and 40°, respectively. The pit exhibits radar backscattering characteristics which notably differ from the other ones in the Magellan radar images²¹ (see examples shown in Fig. 2). In greater detail, the Magellan SAR responses reveal distinct morphological contrasts in the presence of pits as shown in the three example pits displayed in Fig. 2. The pit near Idunn Mons (Fig. 2a) exhibits a pronounced radar shadow coupled with a high-intensity bright return along its eastern margin, consistent with steep, vertically walled topography²¹. In contrast, the pit in Ganiki Planitia (Fig. 2b) shows a weaker and less sharply defined radar shadow, suggesting that it is either shallower or contains a non-uniform infill distribution²¹ compared to the pit near Idunn Mons. The candidate skylight denoted as pit A near Nyx Mons (Fig. 2c and Fig. 1) presents a significantly different response characterized by a well-defined shadow and an asymmetric bright radar return that extends far beyond the pit margin. This asymmetry is identical to that observed in previous radar studies²⁴ in the presence of a collapsed lava tube roof, linking to subsurface voids. The anomalous increase in backscattering can be attributed to the lava tube roof and interior²⁴. According to this interpretation, the pit would result from the collapse of the conduit's roof section, providing access to the subsurface (i.e., empty void).

We estimated the geometric characteristics of pit A (see Fig. 3) by inverting the Magellan radar signals originating from the skylight interior (see Methods). All the hereby reported measurements are associated with an uncertainty of ± 75 m, corresponding to the pixel size in the slant range direction of the Magellan radar dataset (see Methods for details on uncertainty determination). In detail, the skylight measures 1545 m \times 1070 m (major-axis by minor-axis). The estimated collapse depth is about 450 m. The radar signal propagates inside the cave for at least 300 m. This value represents the conduit length for which the radar signal can propagate inside the lava tube before extinguishing. The subsurface conduit has a width that varies

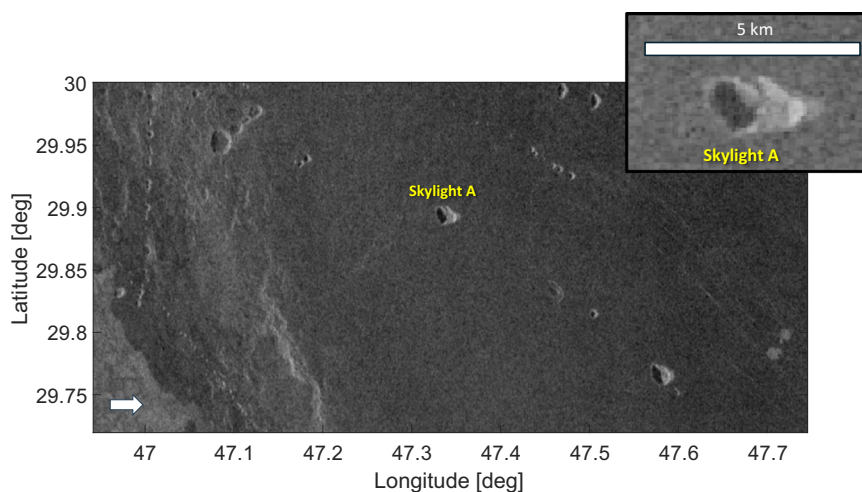


Fig. 1 | Results on a large Venusian skylight providing access to the subsurface. Magellan radar image of Venus (Magellan's Radar System - Full Resolution Radar Left-Look Mosaic, framelet ID: fl29n047) displaying several pit chains

and the identified skylight, marked as A, potentially providing access to the subsurface (i.e., empty void). The white arrow indicates the radar illumination direction.

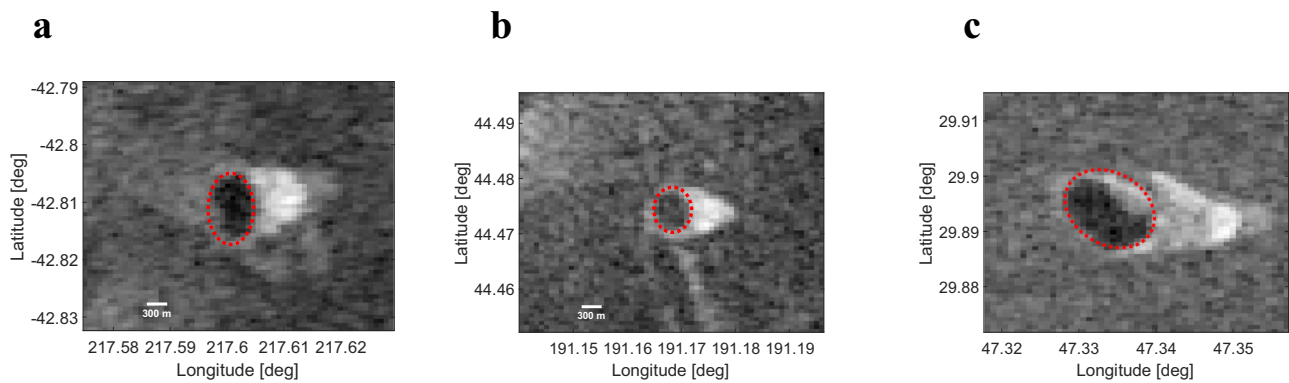


Fig. 2 | Comparison of Magellan SAR radar responses from different pits. a A pit near Idunn Mons. **b** A pit in Ganiki Planitia and **c** the candidate skylight denoted A near Nyx Mons shown in Fig. 1.

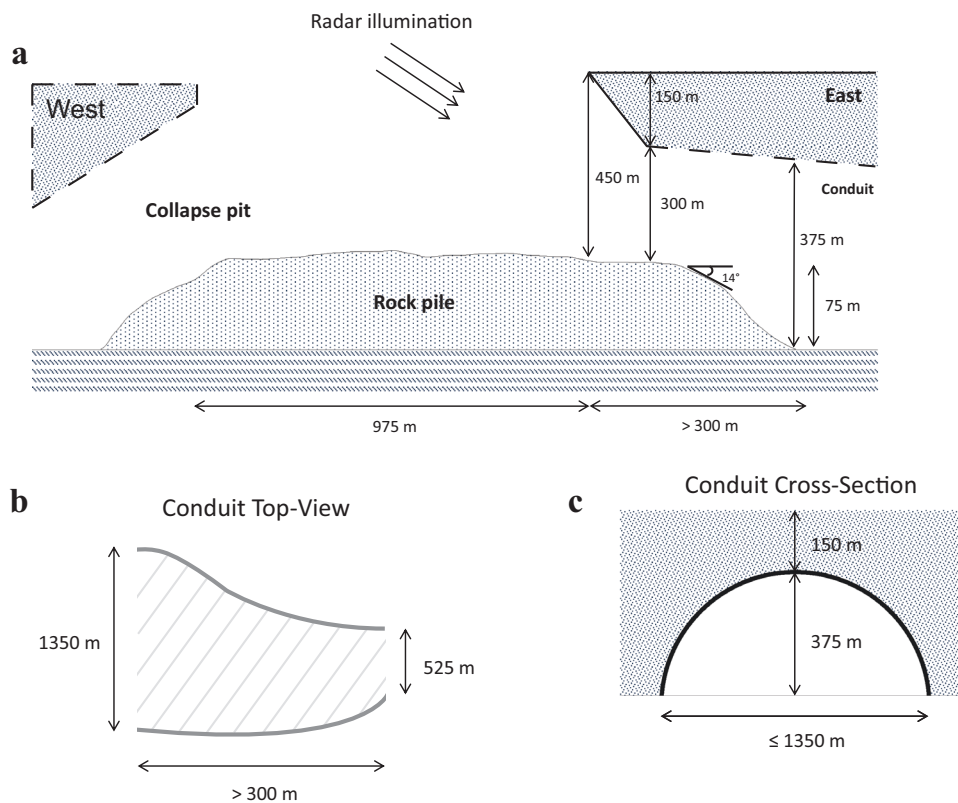


Fig. 3 | Geometric representation of pit A of Fig. 1 based on the Magellan data inversion. The figure reports the **a** side-view, **b** top-view and **c** cross-sectional dimensions of the identified lava tube developing from the skylight. Solid lines

indicate what is observed by the radar. The rock pile originated from the roof collapse. Dashed lines represent geometrical hypotheses based on typical conduit shapes on Earth².

between 1350 m near the skylight and 525 m when reaching the maximum radar visibility point. The average width is equal to 937.5 m. Note that this conduit width may underestimate the true value as it depends on the points of intersection between the conduit's curvature and the oriented electromagnetic waves transmitted from the radar's acquisition position¹⁴. The lava tube roof thickness is estimated to be about 150 m. The cavity height measured inside the hypothesized conduit is ~375 m. As represented in Fig. 3, we hypothesize the presence of a rock pile on the pit floor, originating from the roof collapse. The rock pile slopes down inside the conduit with an estimated angle of ~14°. The cavity height measured from the top of the rock pile is about 300 m. The East-to-West radar data was not acquired over the target area. Therefore, it is not possible to determine the characteristics of the lava tube below the West wall.

We interpret the pit A to belong to a winding (sinuous) collapse chain originating northwest and progressively descending southeast (see Supplementary Fig. 1b). The Magellan altimetry data²⁹ indicate that the surface slopes toward the southeast from pit A (see Supplementary Fig. 1c). This trend supports the idea that, if associated with a sinuous collapse chain, pit A orientation aligns with downhill topography. This is an additional indicator of a lava tube system⁴. It is worth noting that the Magellan data altimetric vertical uncertainty and low horizontal spatial resolution limit our ability to resolve small topographic variations. As lava tubes typically form sinuous chains of collapses predominantly oriented along the direction of the tube², we can infer that the identified potential lava tube is likely to span a length of at least 45 km below the surface. We have evidence that there is at least one section of the conduit that does not show any collapse. It has a length of 13 km

corresponding to the paths from A to B (see Supplementary Fig. 1). The other pits belonging to the chain denoted as B, C, and D show no evidence of direct subsurface access as they have a radar response very similar to the one attributable to skylights with blocked conduit entrance as observed on Earth analogs²⁴. The access to the conduit in these pits is likely to be occluded by the deposit of collapse material.

Morphometric comparison of planetary lava tube collapses

Pit craters that likely originated from the collapse of a lava tube roof have been identified on Mars^{2,10,11,30} and the Moon^{2,12,14,15,31}. Sauro et al.² conducted a morphometric analysis on potential planetary lava tubes, by selecting candidate collapse chains in the lunar regions of Marius Hills and Gruithuisen, and in the martian regions of Arsia, Olympus and Hadriaca volcanoes; the analysis also included a set of skylights located in the known terrestrial lava tube systems of Corona (Spain), Kazamura (Hawai'i) and Undara (Australia). In comparison to the results of Sauro et al., the size of Venusian pit A (major-axis by minor-axis) is in line with what has been observed on the Moon², but larger than what has been identified on Mars, which, in turn, exceeds the size observed for terrestrial cases². The estimated collapse linear volume for pit A (see “Methods”) is equal to $7.56 \times 10^5 \text{ m}^3$. This value is in agreement with lunar observations², while it is larger than the linear volumes measured on Mars² (which are in the order of 10^4 m^3) and on the Earth (which are in the order of 10^1 – 10^2 m^3). The asymmetry ratio for pit A (see “Methods”) is 2.38. Interestingly, well-known lunar skylights, that may provide access to the subsurface, such as Marius Hill Pit, have combined values² of asymmetry ratio and linear volume similar to the ones we measured for Venus’ pit A.

Comparison between Venusian and terrestrial lava tubes radar response

To further validate our results, we compare the radar backscattering response of A with the one of a previously studied lava tube’s

skylights on Earth. Situated in the northern part of Lanzarote, Spain, the Corona volcano has created one of the Earth’s most extensive lava tube systems that displays several collapse pits³². The Corona lava tube spans a length of ~7.6 km (with a total cave development of about 9.7 km, including side branches and upper levels) and exhibits cave sections that reach widths³² of up to ~28 m. This remarkable network comprises multiple skylights and large collapses along the path of the lava tube. With an estimated minimum length of 45 km and a width that is greater than 1 km, the hypothesized Venusian lava tube notably exceeds the dimensions of the Corona system. Nonetheless, the largest lava tubes on Earth, like the one at Corona, are considered as highly valuable analogs to their extraterrestrial counterparts³².

The Corona lava tube system has been subject of an extensive study with spaceborne SAR systems to infer the lava tubes characteristics near collapse pits²⁴. Figure 4a, b reports the SAR and optical images of a previously studied²⁴ collapsed lava tube’s roof (known as *Jameo Agujerado*) providing access to the subsurface. In Fig. 4a, the radar image is superimposed on the 3D Lidar scans and drone photogrammetry of the surface and the subsurface²⁴. The radar image of *Jameo Agujerado* shows backscattering features that are strikingly similar to the radar responses observed for pit A on Venus (see Fig. 1 and Fig. 4a). This comparison shows that both cases are characterized by a typical lava tube response characterized by a well-defined shadow and an asymmetric bright radar return that extends far beyond the pit margin (see also Fig. 2). This further provides evidence that A is a collapsed lava tube section (i.e., skylight) providing access to the subsurface. Figure 4c shows an image of the eastern entrance (the one being imaged by the radar) of *Jameo Agujerado*. We hypothesize that the entrance to the lava tube conduit departing from pit A resembles the one of *Jameo Agujerado* although at a very different spatial scale (hundreds of meters on Venus versus tens of meters on Earth).

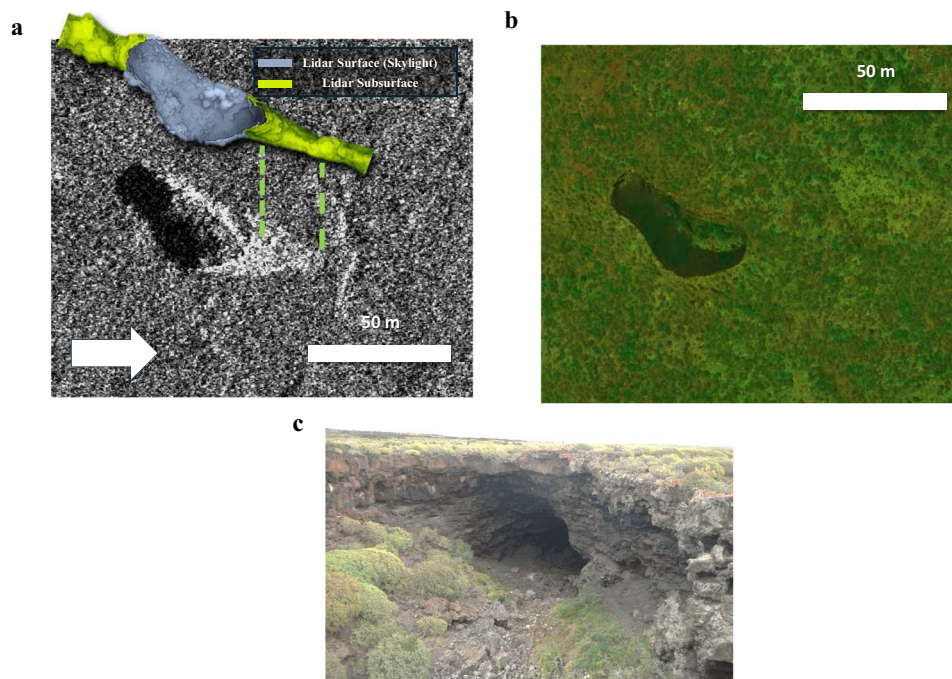


Fig. 4 | Terrestrial analog of Venusian lava tubes. **a** Capella Space SAR image of the terrestrial analog (*Jameo Agujerado*, 29.165489N–13.453964E, Lanzarote, Spain) with the 3D Lidar scans and drone photogrammetry of the surface and the subsurface (Image adapted from ref. 24). The anomalous increase of the radar image brightness near the collapse point (i.e., skylight) originates from the tube interiors and provides information on its morphology. **b** Satellite optical Image of *Jameo*

Agujeredo (WorldView-3 satellite, © Microsoft, Bing Maps, and its data providers). **c** Image (© Primož Jakopin, id: PJ29759) of the eastern entrance (the one being imaged by the radar in Fig. 4a) of *Jameo Agujerado*. The white arrow indicates the radar illumination direction. The comparative analysis of the radar images (see Fig. 1 and Fig. 4a) suggests that the collapse pit marked as A may be a skylight providing access to a lava tube interior.

Discussion

The radar response observed for pit A is unique to empty and accessible subsurface conduits near a skylight. This observation is in line with theoretical modeling of SAR imaging of subsurface cavities from skylights^{14,24,33} and with the comparison between the results obtained on Venus with lava tube terrestrial analog SAR imaging data. The identified candidate skylight is located over an area that based on radar backscattering appears to be topographically smooth at the spatial scale and wavelength of Magellan SAR data. Accordingly, we can rule out that the bright anomalies in SAR images are attributable to surface roughness. Previous studies have demonstrated that the methodology is not adversely affected by surface layover for small to moderate topographic variations, such as those present in this case^{14,21,24,33} (see Supplementary Fig. 1c).

An alternative hypothesis for the genesis of A is that it is a collapse pit with steep vertical internal walls with no subsurface access (e.g., tectonic voids). However, as already stated, the radar backscattering anomaly originating from the interior of these types of pit differs from the one of lava tubes. This is frequently observed along collapse pit chains known to have no subsurface access in Hawaii (Supplementary Fig. 2). Another type of geologic feature that could be potentially ambiguous with collapsed conduits in a SAR image is volcanic vents. In this case, as illustrated by the Hawaii analog (Supplementary Fig. 3), the radar response resembles the one of a collapse pit with steep internal walls. This is evidenced by a pronounced radar shadow and a high-intensity bright return along the eastern margin. Yet it also shows features reminiscent of a lava tube radar response, such as slight elongation whereas lacking the characteristic asymmetry typically associated with horizontally continuous lava tube conduits radar response. The hypothesis of an impact crater is also very unlikely as there is no evidence of ejecta deposits around the features. These deposits tend to increase the radar backscattering uniformly around the feature^{34,35}. Moreover on Venus such deposits typically appear in Magellan radar images as diffuse, high-backscatter regions that extend outward from the crater rim³⁶. This type of response is substantially different than what we observe for pit A. In addition, the small number of impact craters observed on Venus with a diameter below 2 km³⁶ makes the hypothesis even more unlikely.

Another relevant hypothesis is pit chains produced in association with dyke swarms, as these chains on Venus are frequently interpreted in this latter context^{22,37}. A relevant terrestrial analog example is from the Kollóttadyngja lava shield in the Northern Volcanic Zone of Iceland, where a 1.7 km-long chain of collapse pits, up to about 150 m wide and about 50 m deep, has been linked to the Askja fissure swarm³⁸. The chain is interpreted as having formed by collapse into a subsurface pipe generated by the horizontal component of a dyke intrusion beneath the shield. The radar response of these dyke-induced pits resembles that of typical Venusian pits with no horizontal continuation (Supplementary Fig. 4). Therefore, the observed radar signature is most consistent with the interpretation that pit A represents a lava tube roof collapse into an underlying void with horizontal continuation. In general, laterally propagating magmatic dykes can separate overlying strata and create void spaces. If the overlying material is sufficiently thin, localized collapse may occur, forming a pit that connects to a horizontal magmatic pathway. The analyzed terrestrial SAR data favors the lava tube hypothesis. However, given the limited dataset of terrestrial analogs with SAR signatures showing both dike-related collapse and horizontal cavity development, we cannot completely rule out the possibility that pit A and the empty conduits at its base formed through dyke intrusion.

The detected lava tube width and height is larger than the ones theorized on Mars² and on the upper range for what has been hypothesized and detected on the Moon^{2,14}. This finding is not surprising considering the presence of lava channels on Venus that are larger and longer than those observed on other planets²³. The origin of lava tubes

on Venus from overcrusting of lava channels is plausible in light of both pre- and post-Magellan analyses^{23,39–42}. Firstly, the study of lava flow morphologies on Venus suggests the presence of low-viscosity basaltic lava^{23,39,40}, which is responsible for the formation of terrestrial lava tubes. Secondly, it has been observed that Venus' physical and atmospheric parameters could favor the formation of lava tubes from overcrusting²³. Indeed, Venus has a lower gravity and a denser atmosphere with respect to Earth, which would result in the rapid creation of a thick insulating crust soon after the flow leaves its vent^{41,42}. This behavior would then favor the development of tube-fed lava flows⁴¹.

No information is currently available regarding the structural stability of lava tubes on Venus. The critical factors influencing their stability are the thickness of the tube's ceiling, the lava tube cross-section, and the tensile strength of the lava material⁴³. The surface of Venus experiences significantly higher temperatures and pressures than Mars or the Moon. These extreme conditions may influence the morphology and stability of the tube. Lunar lava tubes having a width of about 1 km, similar to the Venusian one characterized in this paper, are reported in the literature⁴³ to be stable for roof thicknesses above 100 m. Lava tubes with small width-to-height ratios (e.g., 1:1 or 3:1) are more stable than more elliptical ones⁴³ (e.g., 6:1 or greater). For pit A, we measure a width-to-height ratio of about 3:1 near the skylight and of about 1.4:1 for the maximum radar visibility point inside the cavity (see Fig. 3).

We were able to locate a large skylight providing access to a potential lava tube on Venus which is also likely accessible. However, the Magellan pixel resolution of 75 m/pixel may have excluded most collapsed lava tubes from our analysis as they are not visible in the acquired images. This suggests that additional skylights, and hence entrances to lava tubes, may remain undetected across other regions of Venus. Accordingly, the results of this paper are also of interest for upcoming missions to Venus such as EnVision⁴⁴ and VERITAS (Venus Emissivity, Radio Science, InSAR, Topography, and Spectroscopy)⁴⁵. Both spacecraft will carry SAR imaging systems operating in S-band and X-band, respectively. The planned resolution for those systems is of about 15–30 m, thus they can greatly enhance the search for skylights. Moreover, EnVision will carry on-board the Subsurface Radar Sounder (SRS)⁴⁶, an orbital ground penetrating radar capable of penetrating up to few hundred meters in the Venus subsurface. Our discovery on potential Venusian lava tubes could be further investigated by such an instrument which could potentially detect intact lava tubes far from the collapse point.

Methods

Radar model and conditions for the detection of the interior of lava tubes

We consider a SAR sensor operating from orbit. We assume that after focusing the system range and azimuth resolutions are better than the cavity width w . The radar received power P_R is directly proportional to the radar backscattering coefficient σ^0 . The value of P_R is given by²⁴:

$$P_R(\theta) = \frac{K\sigma^0(\theta)}{R^4}. \quad (1)$$

The system constant K in the equation depends on factors such as the transmitted power, the antenna gain, and other relevant parameters. The variable R denotes the slant range. The term *clutter* refers to all unwanted radar echoes that have the potential to obscure the desired signal. In the SAR image, the cavity interior (which is the signal of interest) near a collapse point can be detected if the radar echo power originating from the cavity is larger than the echo power arising from the surface (i.e., *clutter*) for the same image pixel. This is considering the cavity interior and surface scattering points at the same slant range that results in the superimposition of two radar echoes. Therefore, the cavity can be detected only when the radar cross

section of the cavity interior σ_c^0 is greater than that of the surface σ_s^0 (i.e., $\sigma_c^0(\theta_c) > \sigma_s^0(\theta_s)$) for any given pixel. Here, θ_c and θ_s represent the local incidence angles inside the cavity and over the surface, respectively, for each pixel in the image.

Radar model for the determination of skylight and lava tubes geometric parameters

The lava tube interior is illuminated if the radar look angle θ_L satisfies the following condition^{21,24} (see Supplementary Fig. 5):

$$\theta_L \leq \text{atan}\left(\frac{D_1}{h_t}\right) \tag{2}$$

where D_1 and h_t are the pit diameter (range direction) and the cavity roof thickness, respectively. This implies that θ_L should be sufficiently low to allow the radar signal to propagate inside the lava tube, rather than being solely reflected by the cavity roof exposed by the skylight. The collapse depth $h = h_t + h_c$ is estimated as (see Supplementary Fig. 5):

$$h = h_t + h_c = \Delta R_{g,1} \sin \theta_l \cos \theta_L \tag{3}$$

where $\Delta R_{g,1}$ is the ground range interval of the radar shadow cast from the pit's edge, h_c is the cavity height measured from the top of the rock pile and θ_l is the radar incidence angle. The radar signal propagation P_1 inside the lava tube is equal to²⁴:

$$P_1 = (\Delta R_{g,2} - \Delta R_{g,3}) \sin \theta_l \sin \theta_L \tag{4}$$

where $\Delta R_{g,2}$ is the ground range extent of the radar anomaly originating from the lava tube interior measured from the relevant pit edge and $\Delta R_{g,3}$ is the ground range interval measured between the reflection from the pit's edge and the first reflection from the roof (see Supplementary Fig. 5). The radar signal propagation inside the lava tube can be also measured with reference to the pit's edge. In this case, the measurement is denoted as P_2 and it is estimated to be:

$$P_2 \leq \Delta R_{g,2} \sin \theta_l \sin \theta_L \tag{5}$$

The maximum depth H_t based on radar signal propagation inside the cavity is equal to:

$$H_t = h_c + h_{pile} + h_t \geq \Delta R_{g,2} \sin \theta_l \cos \theta_L \tag{6}$$

The roof thickness h_t could be estimated in case of vertical roof wall as:

$$h_t = \frac{\Delta R_{g,3} \sin \theta_l}{\cos \theta_L} \tag{7}$$

However, the unknown inclination of the roof wall makes it impossible to reliably estimate its thickness through equations. Indeed, when the roof wall is not vertical, the previous equation could yield an overestimation of the real value. It is possible to obtain an approximation of the inclined roof thickness as:

$$h_t = \Delta R_{g,3} \sin \theta_l \cos \theta_L \tag{8}$$

Nonetheless, in this case, the obtained value may represent an underestimate of the real one.

Therefore, due to the uncertainty about the actual geometry of the cavity roof, the thickness h_t has been estimated numerically, starting from the knowledge of the slant range interval measurement

$\Delta R_{g,3} \sin \theta_l$ as follows:

$$h_t = \text{argmin}_{y_p} \left\{ |\Delta R(x_p, y_p) - \Delta R_{g,3} \sin \theta_l| \right\} \tag{9}$$

where the parametric slant interval measurement $\Delta R(x_p, y_p)$ as function of the roof cartesian reflection point (x_p, y_p) is equal to:

$$\Delta R(x_p, y_p) = R_1 - R_0 = \sqrt{(h_s - y_p)^2 + (h_s \tan(\theta_L) - x_p)^2} - \sqrt{(h_s)^2 + (-h_s \tan(\theta_L))^2} \tag{10}$$

where h_s is the spacecraft height.

The cavity height H_i within the lava tube is equal to:

$$H_i = (\Delta R_{g,2} - \Delta R_{g,3}) \sin \theta_l \cos \theta_L \tag{11}$$

The cavity width w and the pit major and minor axes, denoted as D_x and D_y , respectively, are directly measured on the image. The lava tube floor slope is estimated as:

$$\theta_s = \text{atan}\left[\frac{H_i - h_c}{P_1}\right] \tag{12}$$

To take into account the Magellan pixel resolution, all the geometric measurements of the conduit have been quantized as follows:

$$\underline{y} = \text{round}\left(\frac{y}{75}\right) \cdot 75 \tag{13}$$

where y is a generic cavity parameter (e.g., h). Accordingly, the measurement uncertainty is equal to ± 75 m.

The collapse linear volume V is equal to²:

$$V = \frac{\pi}{2} h D_y \tag{14}$$

The collapse asymmetry ratio AR is defined as²:

$$\text{AR} = \frac{D_y}{h} \tag{15}$$

Analysis of the uncertainties in the determination of skylight and lava tubes geometric parameters from Magellan data

A radar measurement taken at a slant range resolution equal to $R_s = R_r \sin(\theta_i)$, where R_r is the ground range resolution, has a root-mean-square error δR equal to²¹:

$$\delta R = R_s / \sqrt{2\text{SNR}} \tag{16}$$

Given that, for Magellan's system, $R_s = 88$ m and $\text{SNR} = 8$ dB, a value of 24.77 m is obtained for δR . Thus, we have that the uncertainty due to SNR is lower than the one given by the pixel resolution, which is equal to $p = 75$ m ($\delta R < p$). Knowing the values of the incidence angle, θ_i , and look angle, θ_l , corresponding to the analyzed SAR measurement, we can bound the errors for the different estimated quantities. The pit examined in this paper, namely pit A (see Fig. 3), was imaged by Magellan's SAR system with an incidence angle of 42.4° and a look angle of 40°. Consequently, the following uncertainties can be evaluated for the estimated geometric parameters (see Methods and Supplementary Fig. 5). The estimated collapse depth uncertainty is evaluated as $p \sin \theta_i \cos \theta_l = 38.74$ m. The radar signal propagation uncertainty is equal to $p \sin \theta_i \sin \theta_l = 32.75$ m. The lava tube roof thickness (worst-case overestimation model) uncertainty is equal to

$p \sin \theta_i / \cos \theta_i = 66.02\text{m}$. The cave height uncertainty is computed as $p \sin \theta_i \cos \theta_i = 38.74\text{m}$.

Magellan radar system specifications and image data format

Magellan is a SAR system operating in S-band (2.385 GHz). The transmitted peak power is 325 W and the swath width is 25 km (variable). The Full Resolution Radar Mosaicked images (FMAP) used in this study are full-resolution (75 m/pixel) global mosaics produced by the U.S. Geological Survey from Magellan Full-resolution Basic Image Data Record (F-BIDR) data. FMAP products are reprojected from the radar coordinates (delay-doppler) onto the surface of Venus by using information about the spacecraft location based on a priori predictions and earth-based tracking. For this study, the left-look FMAP mosaic has been employed. The radar resolution ranges from 120 m × 120 m (range × azimuth) to 280 m × 120 m, depending on the spacecraft altitude.

Sentinel 1 radar system specifications and image data format

The SAR images used in this paper were acquired by Sentinel 1. Sentinel 1 is a SAR system operating in C-band (5.405 GHz). The Sentinel 1 Ground Range Detected (GRD) products used in this work encompass focused SAR data that have undergone detection, multi-looking, and projection onto the ground range utilizing an Earth ellipsoid model. The ellipsoid projection of the GRD products is adjusted based on the terrain height. Ground range coordinates refer to the slant range coordinates that have been projected onto the Earth's ellipsoid. The pixel values represent the detected magnitude. The resultant product exhibits an approximately square spatial resolution and square pixel spacing of 10 m × 10 m, with reduced speckle owing to the multi-look processing. The spatial resolution is about 20.5 m × 22.5 m in range and azimuth, respectively.

Capella radar system specifications and image data format

The VHR SAR spotlight image of Lanzarote of size 5 km × 5 km used in this paper was acquired with Capella Space X-band radar systems. The radar central frequency and bandwidth are 9.65 GHz and 500 MHz, respectively. Data has been acquired in HH polarization with a pulse repetition frequency of 10 KHz. After the geocoding and orthorectification, the ground range resolution can vary between 0.5 and 0.8 m depending on the look angle. The azimuth resolution is 0.5 m without sidelobe filtering. The standard look angle range for Capella Space X-Band data is between 25° and 40°. Given the small size (5 km × 5 km) of the considered image, the look angle does not appreciably vary across the imaged scene. No post-processing has been applied to the data. We exploited the GEO (Geocoded Terrain Corrected) data products, in which pixel values contain the radiometrically calibrated intensity in linear scale. The image is multi-looked nine times in the azimuth direction to enhance their radiometric resolution. GEO data products are geocoded and terrain-corrected using a Digital Elevation Model to improve the geolocation accuracy beyond what is achievable with only considering the ellipsoid.

Data availability

The VHR SAR data of Lanzarote used in this study will be released as part of the Capella Space Open Data Program <https://www.capellaspace.com/community/capella-open-data/> under the following user license <https://www.capellaspace.com/customers/product-documentation/data-licensing/>. The Magellan FMAP data used in this study is publicly available on the NASA planetary data system geoscience node at the following address https://ode.rsl.wustl.edu/venus/pagehelp/Content/Missions_Instruments/Magellan/Radar_System/Other_Records/FMAP.htm. The Sentinel 1 GRD data used in this study is publicly available at <https://scihub.copernicus.eu/>. Magellan Altimetry data is publicly available through Java Mission-

planning and Analysis for Remote Sensing (JMARS) at <https://jmars.asu.edu/>.

Code availability

All the relevant analyses on the experimental data were performed using MATLAB ©. Code is available upon request.

References

- Léveillé, R. J. & Datta, S. Lava tubes and basaltic caves as astrobiological targets on Earth and Mars: a review. *Planet. Space Sci.* **58**, 592–598 (2010).
- Sauro, F. et al. Lava tubes on Earth, Moon and Mars: a review on their size and morphology revealed by comparative planetology. *Earth-Sci. Rev.* **209**, 103288 (2020).
- Kempe, S. Volcanic rock caves. In *Encyclopedia of Caves* (pp. 1118–1127). (Academic Press, 2019).
- Valerio, A. Tallarico, A. & Dragoni, M. Mechanisms of formation of lava tubes. *J. Geophys. Res. Solid Earth* **113** (2008).
- Calvari, S. & Pinkerton, H. Lava tube morphology on Etna and evidence for lava flow emplacement mechanisms. *J. Volcanol. Geotherm. Res.* **90**, 263–280 (1999).
- Peterson, D. W., Holcomb, R. T., Tilling, R. I. & Christiansen, R. L. Development of lava tubes in the light of observations at Mauna Ulu, Kilauea Volcano, Hawaii. *Bull. Volcanol.* **56**, 343–360 (1994).
- Kempe, S. (2009). Principles of pyroduct (lava tunnel) formation. In *Proc. 15th International Congress of Speleology* (Vol. 2, pp. 668–674).
- Nesnas, I. A. et al. Moon diver: exploring a Pit's exposed strata to understand lunar volcanism. *Acta Astronaut.* **211**, 163–176 (2023).
- Michalski, J. R. et al. The Martian subsurface as a potential window into the origin of life. *Nat. Geosci.* **11**, 21–26 (2018).
- Cushing, G. E. Candidate cave entrances on Mars. *J. Cave Karst Stud.* **74**, 33–47 (2012).
- Crown, D. A., Scheidt, S. P. & Berman, D. C. Distribution and morphology of lava tube systems on the western flank of Alba Mons, Mars. *J. Geophys. Res. Planets* **127**, e2022JE007263 (2022).
- Greeley, R. Lava tubes and channels in the lunar Marius Hills. *Moon* **3**, 289–314 (1971).
- Blamont, J. A roadmap to cave dwelling on the Moon and Mars. *Adv. Space Res.* **54**, 2140–2149 (2014).
- Carrer, L. et al. Radar evidence of an accessible cave conduit on the Moon below the Mare Tranquillitatis pit. *Nat. Astron.* **8**, 1119–1126 (2024).
- Haruyama, J. et al. Possible lunar lava tube skylight observed by SELENE cameras. *Geophys. Res. Lett.* **36** (2009).
- Wyrick, D. Y. & Buczkowski, D. L. Pit crater chains across the solar system: evidence for subterranean tectonic caves, porosity and permeability pathways on planetary bodies. *J. Geophys. Res. Planets* **127**, e2022JE007281 (2022).
- Wynne, J. J. et al. Planetary caves: a solar system view of processes and products. *J. Geophys. Res. Planets* **127**, e2022JE007303 (2022).
- Saunders, R. S. et al. The Magellan Venus radar mapping mission. *J. Geophys. Res. Solid Earth* **95**, 8339–8355 (1990).
- Bleamaster III, L. F. & Hansen, V. L. Effects of crustal heterogeneity on the morphology of chasmata, Venus. *J. Geophys. Res. Planets* **109** (2004).
- Davey, S. C., Ernst, R. E., Samson, C. & Grosfils, E. B. Hierarchical clustering of pit crater chains on Venus. *Can. J. Earth Sci.* **50**, 109–126 (2013).
- Carrer, L., Diana, E. & Bruzzone, L. Assessing the morphometry of pit craters on venus from orbital synthetic aperture radar data. In: *Proc. IEEE Transactions on Geoscience and Remote Sensing* (IEEE, 2024).
- Ernst, R. E., Grosfils, E. B. & Mege, D. Giant dike swarms: Earth, Venus, and Mars. *Annu. Rev. Earth Planet. Sci.* **29**, 489–534 (2001).

23. Melville, G. P. *Lava Tubes and Channels of the Earth, Venus, Moon and Mars*. Doctoral Dissertation (University of Wollongong, 1994).
24. Carrer, L., Castelletti, D., Pozzobon, R., Sauro, F. & Bruzzone, L. A novel method for hidden natural caves characterization and accessibility assessment from spaceborne VHR SAR images. *IEEE Trans. Geosci. Remote Sens.* **61**, 1–11 (2022).
25. Ivanov, M. A. & Head, J. W. Large volcanoes on Venus: Morphology, morphometry, and stratigraphy. *Icarus* **429**, 116404 (2025).
26. Campbell, Bruce A., Campbell, Patricia G. Geologic Map of the Bell Regio Quadrangle (V–9), Venus: U.S. Geological Survey Geologic Investigations Series Map I-2743, 1 plate, <https://pubs.usgs.gov/imap/2743/> (2002).
27. Sawford, W. C., Ernst, R. E., Samson, C., Davey, S. C. « Pit crater chains in the Nyx Mons Region, Venus ». In *Proc. 46th Lunar and Planetary Science Conference* (Houston, TX, USA, Mar. 16–20, 2015) Coll. « LPI Contribution », vol. 1832 (Lunar and Planetary Institute, 2015).
28. Rogers, P. G. & Zuber, M. T. Tectonic evolution of Bell Regio, Venus: Regional stress, lithospheric flexure, and edifice stresses. *J. Geophys. Res. Planets* **103**, 16841–16853 (1998).
29. Herrick, R. R., Wren, P. JMARS: cCollecting and ingesting data to create a useful scientific analysis tool. In *Proc. 15th Meeting of the Venus Exploration and Analysis Group (VEXAG)* (Vol. 15, No. 2061, p. 8021) (2017).
30. Wyrick, D., Ferrill, D. A., Morris, A. P., Colton, S. L. & Sims, D. W. Distribution, morphology, and origins of Martian pit crater chains. *J. Geophys. Res. Planets* **109** (2004).
31. Wagner, R. V. & Robinson, M. S. Distribution, formation mechanisms, and significance of lunar pits. *Icarus* **237**, 52–60 (2014).
32. Tomasi, I. et al. Inception and evolution of La Corona Lava Tube System (Lanzarote, Canary Islands, Spain). *J. Geophys. Res. Solid Earth* **127**, e2022JBO24056. (2022).
33. Carrer, L., Castelletti, D., Pozzobon, R., Sauro, F. & Bruzzone, L. A Method for the characterization of the interior of pits from single spaceborne SAR images. *IEEE Geosci. Remote Sens. Lett.* **21**, 1–5 (2024).
34. Thompson, T. W., Campbell, B. A., Ghent, R. R., Hawke, B. R. & Leverington, D. W. Radar probing of planetary regoliths: An example from the northern rim of Imbrium basin. *J. Geophys. Res. Planets* **111**, E06S14 (2006).
35. Neish, C. D., Virkki, A. K. The unusual surface texture of venusian impact ejecta. In *Proc. 54th Lunar and Planetary Science Conference 2023* (2023).
36. Schaber, G. G. et al. Geology and distribution of impact craters on Venus: what are they telling us? *J. Geophys. Res. E Planets* **97**, 13257–13301 (1992).
37. Riaz, M., Ernst, R. E. & El Bilali, H. Dyke swarms of Bell Regio, Venus. In *Proc. 54th Lunar and Planetary Science Conference* (Vol. 2806, p. 1510) (2023).
38. Hjartardóttir, Á. R. *The Fissure Swarm of the Askja Central Volcano Doctoral dissertation, M. Sc. Thesis* (University of Iceland, 2008).
39. Wroblewski, F. B., Treiman, A. H., Bhiravarasu, S. & Gregg, T. K. P. Ovda Fluctus, the festoon lava flow on Ovda Regio, Venus: Not silica-rich. *J. Geophys. Res. Planets* **124**, 2233–2245 (2019).
40. Gregg, T. K. P., Sakimoto, S. E. H. Venusian lava flow morphologies: variations on a basaltic theme. In *Proc. Lunar and Planetary Science Conference* Vol. 27. Pages 459 (1996).
41. Head, J. W. & Wilson, L. Volcanic processes and landforms on Venus: theory, predictions, and observations. *J. Geophys. Res.* **91**, 9407 (1986).
42. Gregg, T. K. P. & Greeley, R. Formation of Venusian canali: considerations of lava types and their thermal behaviors. *J. Geophys. Res.* **98**, 873–882 (1993).
43. Theinat, A. K. et al. Lunar lava tubes: morphology to structural stability. *Icarus* **338**, 113442 (2020).
44. Ghail, R. C. et al. VenSAR on EnVision: taking earth observation radar to Venus. *Int. J. Appl. Earth Observ. Geoinf.* **64**, 365–376 (2018).
45. Smrekar, S. et al. VERITAS (Venus emissivity, radio science, InSAR, topography, and spectroscopy): a discovery mission. In *Proc. IEEE Aerospace Conference (AERO)* (pp. 1–20) (IEEE, 2022).
46. Bruzzone, L. et al. Envision mission to Venus: subsurface radar sounding. In *Proc. IGARSS 2020-2020 IEEE International Geoscience and Remote Sensing Symposium* (pp. 5960–5963). (IEEE, 2020).

Acknowledgements

This work was supported by the Italian Space Agency under Grant n. 2022-23-HH.0 “Attività scientifiche per il radar sounder di EnVision fase B1” (CUP: F63C22000650005).

Author contributions

L.C. and L.B. conceived the concepts of the research. E.D. developed the experiments. L.C., E.D. and L.B. analyzed the experimental radar data. L.C. provided the geologic interpretation of the experimental results. L.B. supervised the research and the related funding project. All the authors co-wrote the paper.

Competing interests

The authors declare no competing interests.

Additional information

Supplementary information The online version contains supplementary material available at <https://doi.org/10.1038/s41467-026-68643-6>.

Correspondence and requests for materials should be addressed to Leonardo Carrer or Lorenzo Bruzzone.

Peer review information *Nature Communications* thanks Ian Flynn, Lindsay McHenry, and the other, anonymous, reviewer for their contribution to the peer review of this work. A peer review file is available

Reprints and permissions information is available at <http://www.nature.com/reprints>

Publisher’s note Springer Nature remains neutral with regard to jurisdictional claims in published maps and institutional affiliations.

Open Access This article is licensed under a Creative Commons Attribution-NonCommercial-NoDerivatives 4.0 International License, which permits any non-commercial use, sharing, distribution and reproduction in any medium or format, as long as you give appropriate credit to the original author(s) and the source, provide a link to the Creative Commons licence, and indicate if you modified the licensed material. You do not have permission under this licence to share adapted material derived from this article or parts of it. The images or other third party material in this article are included in the article’s Creative Commons licence, unless indicated otherwise in a credit line to the material. If material is not included in the article’s Creative Commons licence and your intended use is not permitted by statutory regulation or exceeds the permitted use, you will need to obtain permission directly from the copyright holder. To view a copy of this licence, visit <http://creativecommons.org/licenses/by-nc-nd/4.0/>.

© The Author(s) 2026